Antarctic Science 21(4), 401–409 (2009) © Antarctic Science Ltd 2009 doi:10.1017/S0954102009001989

Study of surface energy and mass balance at the edge of the Antarctic ice sheet during summer in Dronning Maud Land, East Antarctica

H.S. GUSAIN*, K.K. SINGH, V.D. MISHRA, P.K. SRIVASTAVA and A. GANJU

Snow & Avalanche Study Establishment, Manali, India
**gusain_hs@yahoo.co.in*

Abstract: This study estimates energy and mass balance at the edge of the Antarctic ice sheet close to a non-glaciated area. An automatic weather station was installed on the ice sheet, near an ice free area of Schirmacher Oasis in Dronning Maud Land, East Antarctica. Hourly snow-meteorological parameters were recorded and observed during the summer of the year 2007–08. Hourly radiative and turbulent energy fluxes were estimated at the ice surface. An ultrasonic sensor was used to measure accumulation or ablation at the glacier surface. Ground Penetrating Radar was also used to measure the changes in ice thickness at the observation point. The net radiative flux was the main heat source and the latent heat flux was the main heat sink for the ice sheet with seasonal average values of 98 W m^{-2} and -86.7 W m^{-2} respectively. There was a high ablation rate for the ice sheet near the non-glaciated area with a seasonal mean of 0.0172 m w.e. per day. Over the period 10 November 2007–7 February 2008 the mass balance was -1.53 m w.e. Good correlation ($r^2 = 0.97$) was observed between estimated and observed hourly ablation of the glacier. Sublimation and melt processes contributed 16.5% and 83.5% respectively to the net summer ablation.

Received 5 August 2008, accepted 2 February 2009

Key words: net radiative flux, non-glaciated area, Schirmacher Oasis, turbulent fluxes

Introduction

The contribution of various physical processes at the snow/ice surface to the energy budget of the ice sheet is different in different parts of the Antarctic. Quantification of these physical processes governing energy exchange between the surface and the atmosphere can contribute towards a better understanding of the stability of the ice sheet. Extensive research has been carried out on the surface energy balance and the surface energy fluxes of the Antarctic ice sheet at various localities (e.g. Bintanja & Van den Broeke 1994, 1995a, 1995b, Bintanja 1995, 1999, Lewis *et al*. 1998, Schneider 1999, Mishra 1999, Braun & Schneider 2000, King *et al*. 2001, Srivastava 2002, Van den Broeke *et al*. 2005, 2006, Gusain *et al*. 2008, Hoffman *et al*. 2008).

The mass balance of the ice sheet has received considerable attention in recent years both because of interest in the contribution that Antarctic ice mass changes could make to variations in global sea level (King & Turner 1997) and because the ice sheet is sensitive to climate change. Mass balance studies have been carried out on different parts of the ice sheet, ice shelves and glaciers of Antarctica (Vaughan *et al*. 1999, Bintanja & Reijmer 2001, Van den Broeke *et al*. 2004, Fountain *et al*. 2006, Genthon *et al*. 2007), but little information is available on energy and mass balance of the Antarctic ice sheet near the Schirmacher Oasis.

Recently it has been noticed that non-glaciated coastal areas can be significant energy sources for the atmosphere when they are exposed during summer (Choi *et al*. 2008) and more attention may need to be paid to the role of these areas. In this paper we present the results of a surface energy and mass balance study at the edge of Antarctic ice sheet close to Schirmacher Oasis during the summer period 2007–08.

Study area and data observations

Schirmacher Oasis (70°44'–70°46'S, 11°24'–11°54'E), lies about 70 km inland from Prinsesse Astrid Kyst in Dronning Maud Land, East Antarctica. The oasis is a rocky area with low-lying hills (*c*. 50–200 m high) with the East Antarctic Ice Sheet lying to the south. A Sutron automatic weather station (AWS) was installed on the ice sheet at 70°46'05.1"S, 11°42'12.2"E, at an altitude of 142 m a.s.l., *c*. 10 m from the ice free area of the oasis. The thickness of the ice sheet at the AWS installation point was around 4 m. The observation site is shown in Fig. 1. The AWS records hourly observations of air temperature, relative humidity, wind speed, wind direction, incoming solar radiation, reflected solar radiation, pressure and glacier surface temperature. Snow depth was also recorded using an ultrasonic snow depth sensor (Table I). All the sensors of AWS were powered by 100 ampere-hour battery, which was recharged by a solar panel. Cloud amount and type were recorded conventionally in hourly observations at the Indian Research Station 'Maitri', nearly 1 km from the study site.

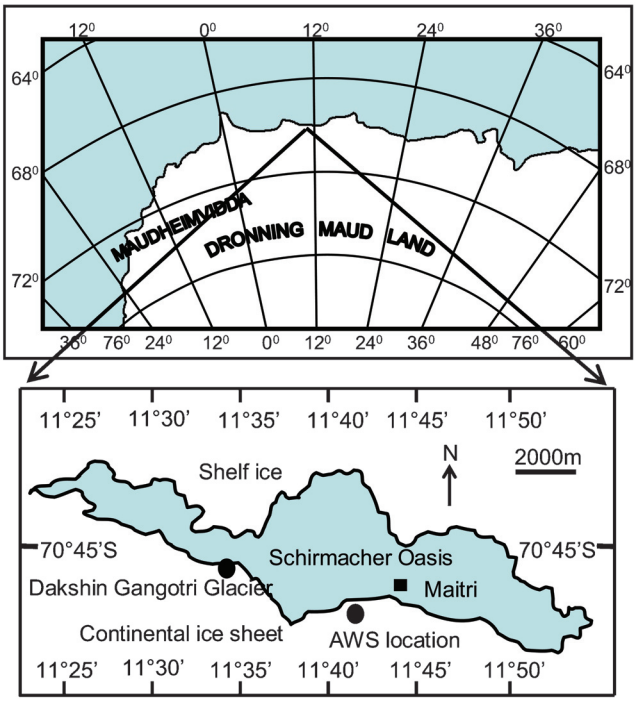

Fig. 1. Observation site.

Methodology

The surface energy balance of a glacier is expressed as:

$$SHW_{net} + LW_{net} + SHF + LHF + G - \Delta Q = 0 \quad (1)$$

where

$SHW_{net} = SHW\downarrow - SHW\uparrow$
$LW_{net} = LW\downarrow - LW\uparrow$
$SHW\downarrow$ = Incoming shortwave radiation flux
$SHW\uparrow$ = Outgoing shortwave radiation flux
$LW\downarrow$ = Incoming longwave radiation flux
$LW\uparrow$ = Outgoing longwave radiation flux
SHF = Sensible heat flux
LHF = Latent heat flux
G = Subsurface conductive heat flux
ΔQ = Energy available for melt

All the terms of Eq. (1) are estimated at the surface and defined positive when directed towards the surface. Net change in the energy storage of the glacier is defined by the net radiative flux, the turbulent fluxes (SHF and LHF) and the subsurface heat flux.

Net radiative flux

Net radiative flux is the sum of downwelling global solar radiation, reflected solar radiation, outgoing terrestrial longwave radiation and downwelling longwave radiation emitted by clouds and atmospheric gases. The proportion of the downwelling solar radiation which is absorbed at the surface or beneath the surface is called the net shortwave radiation and is given by

$$SHW_{net} = SHW\downarrow - SHW\uparrow = SHW\downarrow (1 - \alpha) \quad (2)$$

where α is albedo of the surface. Here the radiative fluxes inside the ice were not measured or modelled, and all radiation is assumed to be absorbed at the surface.

The downwelling longwave radiation component ($LW\downarrow$) is dependent on the vertical distribution of temperature, vapours in the atmosphere and the optical properties of cloud if present. This $LW\downarrow$ is estimated using a model developed by Prata (1996). The model computes emissivity of the atmosphere (ϵ_m) dependent on precipitable water content (w) and performs well in a dry atmosphere:

$$LW\downarrow = \epsilon_m \sigma T_a^4 \quad (3)$$

$$\text{where } \epsilon_m = 1 - (1 + w) \exp\{-(1.2 + 3.0w)^{1/2}\} \quad (4)$$

$$\text{and } w = 46.5\ (e_a/T_a) \quad (5)$$

e_a is vapour pressure (Pa) and T_a the absolute temperature measured at 1.5–2.0 m height above surface.

$LW\uparrow$ is the outgoing terrestrial longwave radiation and computed from the Stefan-Boltzmann Law as the snow/ice surface is assumed as a nearly perfect black body in the longwave portion of the electromagnetic (EM) spectrum. The surface emissivity of snow and ice is assumed to be unity (Bintanja & Van den Broeke 1994). Outgoing

Table I. Sensor specifications of automatic weather station.

Sensor	Range	Accuracy	Type
Air temperature	-50°C to +50°C	±0.3°C	Campbell Scientific 41372V-90
Air pressure	400 to 1100 mBar	0.5 mBar	Anika PTB210B2A1B
Relative humidity	0–100%	±3% from 0–90% ±4% from 90–100%	Campbell Scientific 41372V-90
Wind speed	0–50 m s^{-1}	±0.3 m s^{-1}	RM Young 05103
Wind direction	360 degree	±3 degree	RM Young 05103
Albedometer	305 to 2800 nm	±10%	Kipp & Zonen CM3
Snow surface temperature	-50°C to +50°C	±0.1°C from –10°C to +10°C ±0.3°C elsewhere	Everest 4000
Snow depth	Up to 10 m	±1.0 cm	Campbell Scientific SR50

https://doi.org/10.1017/S0954102009001989 Published online by Cambridge University Press

longwave radiation can be computed as:

$$LW\uparrow = \epsilon_s \sigma T_s^4 \quad (6)$$

where σ is the Stefan-Boltzmann constant (5.67×10^{-8} W m^{-2} K^{-4}), T_s the radiative temperature of the surface in kelvins and ϵ_s the surface emissivity.

On a cloud free day the net longwave radiation absorbed by the glacier surface is:

$$LW_{net} = LW\downarrow - LW\uparrow \quad (7)$$

$$= \epsilon_m \sigma T_a^4 - \epsilon_s \sigma T_s^4 \quad (8)$$

Cloud affects the net longwave radiation significantly. The main role of cloudiness is to reduce the loss of longwave radiation. If N is the amount of cloudiness in terms of fraction of sky covered, then

$$LW_{net} = (\epsilon_m \sigma T_a^4 - \epsilon_s \sigma T_s^4)(1 - KN) \quad (9)$$

where the coefficient K depends on type and height of clouds. Experimental values reported by US Army Corps of Engineers (1956) are (Upadhyay 1999):

$$K = 0.76 \text{ for low clouds}$$
$$= 0.52 \text{ for medium clouds}$$
$$= 0.26 \text{ for high clouds}$$

Net radiative flux in the model is computed as:

$$R_{net} = SHW\downarrow(1 - \alpha) + (\epsilon_m \sigma T_a^4 - \epsilon_s \sigma T_s^4)(1 - KN) \quad (10)$$

Turbulent fluxes

Sensible heat flux (SHF) and latent heat flux are the turbulent energy fluxes. The vertical turbulent sensible heat flux is expressed in terms of wind speed and temperature (Ambach & Kirchlechner 1986, Paterson 1994) as follows:

$$SHF = (C_p \rho_0 / P_0) K_n P u (T_a - T_s) \quad (11)$$

$$K_n = k^2 / [\log(z_a / z_0)]^2 \quad (12)$$

where ρ_0 is the density of air (1.29 kg m^{-3}) at the standard atmospheric pressure P_0 (1.013×10^5 Pa), K_n is a dimensionless transfer coefficient, P is the mean atmospheric pressure (Pa) at measuring site, u and T_a are the measured wind speed (ms^{-1}) and air temperature (K) at a height of 2 m above the glacier surface respectively, k is von Karman's constant (0.41), z_a is the sensor height above ground (2 m) and z_0 is aerodynamic roughness length. The accuracy of the bulk method depends on the accuracy with which z_0 can be specified and an order of magnitude increase in z_0 will more than double the value of the turbulent fluxes (Brock *et al*. 2000). Aerodynamic roughness values recorded over melting glacier surfaces vary over three orders of magnitude, in the 0.1–10 mm range. At high latitudes, the recorded z_0 range is five orders of magnitude from 0.001 to 10 mm (Brock *et al*. 2006). Whilst a value of z_0 as low as 3.10^{-6} has been observed over an Antarctic blue ice surface (Bintanja & Van den Broeke 1995b). Bintanja & Van den Broeke also studied the relationship between aerodynamic roughness length and roughness lengths of momentum, heat and moisture over smooth ice and snow surfaces. They observed that the scalar roughness lengths seem to be approximately equal to z_0 for a wide range of low roughness Reynolds numbers, despite the frequent occurrence of drifting snow (Bintanja & Van den Broeke 1995a). In the present study z_0 was not measured and a value of 1 mm was chosen to provide the best model agreement with measurements of ablation.

Latent heat flux (LHF) is an important component of the surface energy budget and carried by turbulent transport in the atmospheric boundary layer. By analogy with the sensible heat flux, the latent heat flux is given by:

$$LHF = L_v (0.623 \rho_0 / P_0) K_n u (e_a - e_s) \quad (13)$$

where L_v is the latent heat of vaporization, e_a is the vapour pressure at height z above glacier surface and e_s is the saturated vapour pressure at the glacier surface. Later is a function of the surface temperature and is 611 Pa for a melting surface (Paterson 1994). Ambach & Kirchlechner (1986), and Greuell & Konzelmann (1994), were followed for distinguishing between sublimation and condensation e.g. when (e_a-e_s) is positive, and $T_s = 0$ deg, water vapour condenses as liquid water on the melting glacier surface with $L_v = 2.514$ MJ kg^{-1}, when (e_a-e_s) is negative, there is sublimation with $L_v = 2.849$ MJ kg^{-1}. Also, when (e_a-e_s) is positive and $T_0 < 0$ deg, there is deposition from vapour to solid ice with $L_v = 2.849$ MJ kg^{-1}.

The equations of sensible and latent heat fluxes are applicable for neutral atmospheric conditions. In Antarctica the atmospheric conditions above the ice sheet are rarely neutral and so the equations can be applied with stability corrections for the transfer coefficient K_n in terms of the bulk Richardson number (Ri). For unstable conditions ($Ri < 0$) transfer coefficient is given by $Kw2 = K_n.(1\text{-}10R_i)$. For $Ri = 0$, $Kw2 = K_n$; and for stable conditions ($Ri > 0$), $Kw2 = K_n/(1 + 10\ R_i)$ (Price & Dunne 1976).

Subsurface conductive heat flux

The subsurface conductive heat flux G can be calculated from

$$G = -\lambda (\partial T / \partial x) \quad (14)$$

where λ is thermal conductivity of ice ≈ 2.4 W m^{-1} K^{-1} and $\partial T/\partial x$ is the temperature gradient inside ice. In this study hourly subsurface conductive heat flux was estimated for the top 50 cm of the ice sheet from 20–22 November 2007 using thermistor measurements. For temperature gradient calculation, temperatures were measured at the ice surface and at 50 cm depth of the ice sheet by calibrated thermistors. Hourly values of subsurface conductive heat flux were observed between 0.0–4.8 W m^{-2} and the daily averaged

https://doi.org/10.1017/S0954102009001989 Published online by Cambridge University Press

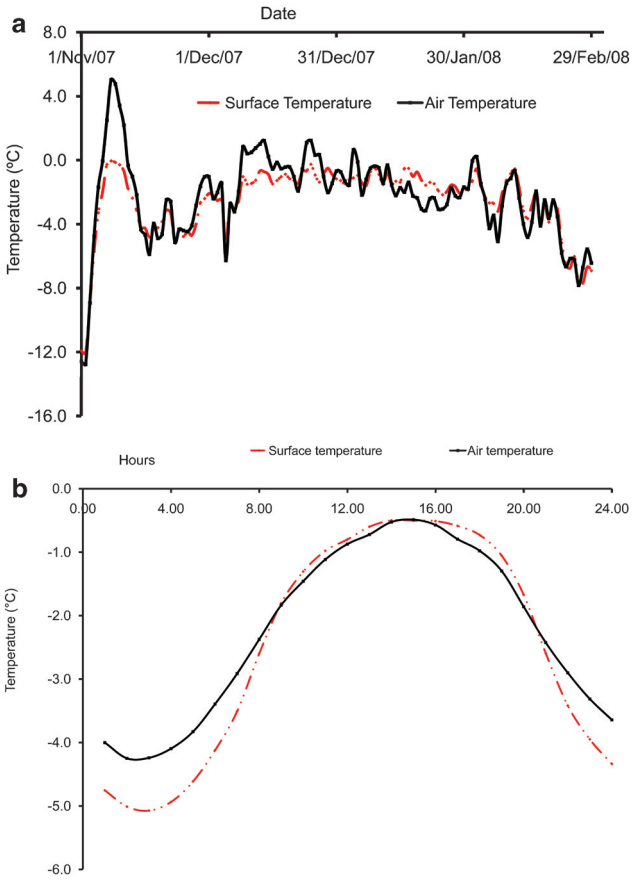

Fig. 2. a. Daily averaged glacier surface temperature and air temperature. **b.** Seasonal mean temperature cycle.

value was less than 1.0 W m^{-2}. As the subsurface conductive heat flux value was small compared to other energy fluxes, it was ignored in the final calculation of the energy balance.

Mass balance

The net energy balance is the net flux into or out of the glacier surface. Positive net energy indicates the gain of

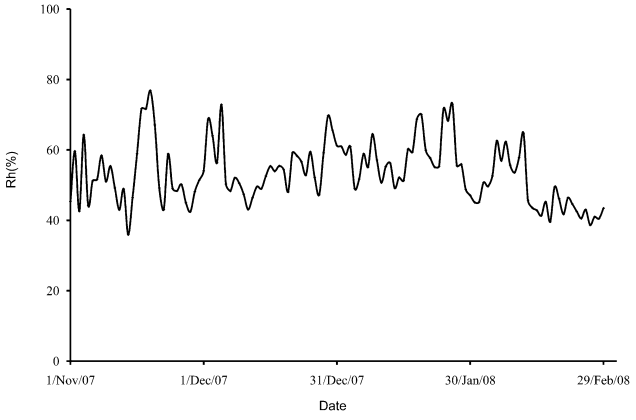

Fig. 3. Daily averaged relative humidity.

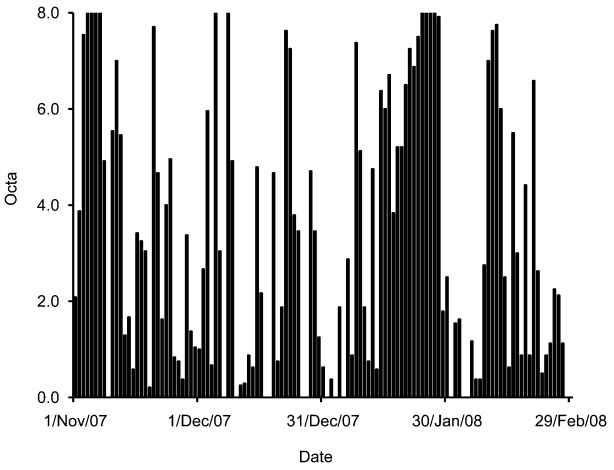

Fig. 4. Daily averaged cloud amount.

energy by the surface, and negative energy indicates the loss of energy from the glacier surface. The energy gained by the surface is the available energy for melt or gain of mass by condensation or deposition, while the energy lost by the glacier surface is used in sublimation/evaporation and cooling of the glacier. In the present study sublimation and melt of the ice sheet is estimated from the latent heat flux and the net energy available for melting. Net estimated ablation of the glacier is the sum of estimated sublimation and estimated melt. Observed ablation of the glacier was recorded hourly using an ultrasonic snow depth sensor. A RAMAC Ground Penetrating Radar (GPR) of 500 MHz frequency was also used to measure the changes in ice thickness during the season.

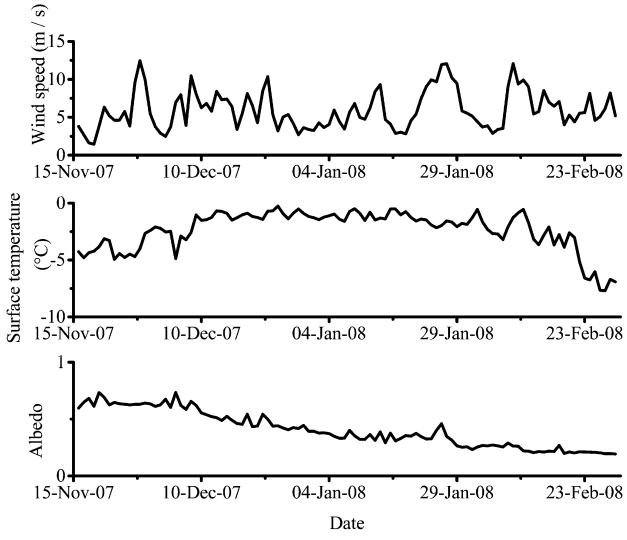

Fig. 5. Variation of daily averages of wind speed, surface temperature and albedo.

https://doi.org/10.1017/S0954102009001989 Published online by Cambridge University Press

Table II. Monthly and seasonal values of various parameters.

Parameter	Nov 2007	Dec 2007	Jan 2008	Feb 2008	Summer season
Air temp °C (mean)	-2.9	-0.8	-1.7	-3.7	-2.2
Surface temp °C (mean)	-3.9	-1.5	-1.3	-3.5	-2.5
Relative humidity % (mean)	52.6	55.3	57.5	47.9	53.3
SWout W m^{-2} (mean)	188	183	93	56	130
SWin W m^{-2} (mean)	281	356	274	243	289
Albedo (mean)	0.67	0.51	0.34	0.23	0.44
Wind speed m s^{-1} (mean)	6.4	5.8	6.3	6.2	6.2
Cloud amount octa (mean)	3.8	2.7	4.3	2.5	3.3
Net SW flux W m^{-2} (mean)	93	173	181	187	159
Net LW flux W m^{-2} (mean)	-59.2	-62.3	-54.0	-68.6	-61
Net radiative flux W m^{-2} (mean)	33.8	110.7	127	118.4	98
Sensible heat flux W m^{-2} (mean)	24	12.4	-9.2	-1.0	6.5
Latent heat flux W m^{-2} (mean)	-82.3	-79.7	-91.9	-92.3	-86.7
Net energy W m^{-2} (mean)	-24.2	43.6	25.8	25.2	17.8
Ice sublimation cm (net)	6*	9	10	2**	27***
Ice melt cm (net)	4*	53	59	21**	137***
Estimated ablation cm (net)	10*	62	69	23**	164***
Observed ablation cm (net)	8*	84	57	18**	167***

* = data from 10–30 Nov 2007, ** = data from 1–7 Feb 2008, *** = season data from 10 Nov 2007–7 Feb 2008.

Results and discussion

Time series of meteorological parameters

Daily averaged meteorological conditions during the observation period 1 November 2007–29 February 2008 are shown in Figs 2–5. Mean monthly values of the parameters are shown in Table II. Daily averaged glacier surface temperature varied from -12°C to 0°C, with aseasonal mean of -2.5°C and daily averaged air temperature varied from -13°C to 5°C, with a seasonal mean of -2.2°C (Fig. 2). The hottest day of the summer was 8 November 2007 with a maximum hourly mean air temperature of +6.5°C at 09h00. Seasonal average values of glacier surface temperature and air temperature for 24 hours are shown in Fig. 2. From 08h00 to 20h00 the glacier surface was warmer than air above the surface.

Hourly relative humidity varied from 21–97% and daily averages varied from 36–77% (Fig. 3) during the observation period with seasonal mean of 53%.

Hourly averaged wind speed varied from 0.3 m s^{-1} to 20.0 m s^{-1} and daily averaged wind speed varied from 1.5 m s^{-1} to 16.0 m s^{-1} (Fig. 5) with seasonal mean of 6.2 m s^{-1}. A constant monthly mean wind speed of around 6.0 m s^{-1} was observed for all the months. The last week of January was windier compared to other weeks with average hourly wind speed of approximately 10 m s^{-1}.

Most of the days were partly cloudy to cloudy (Fig. 4). Mean monthly cloud amount varied from 2.5–4.3 octa with seasonal mean of 3.3 octa. January was the most cloudy month and February the least.

Daily averaged incoming shortwave radiation varied from 50 W m^{-2} to 432 W m^{-2}, while outgoing shortwave radiation varied from 11 W m^{-2} to 250 W m^{-2}. In the daily radiation cycle, the maximum incoming shortwave radiation was at 11h00 hours. Albedo values of the glacier surface are interesting as a decreasing trend was noted during the observation period (Fig. 5). Mean monthly albedo varied from 0.67–0.23 with the seasonal mean value of 0.44. This indicates more absorption of the shortwave radiation at the glacier surface as the season progresses. As albedo values of the glacier surface depend on a number of parameters (surface characteristics, cloud cover, solar zenith angle etc.), there may be various reasons for this phenomenon. Glacier surface characteristics play an important role in albedo variation. Figure 5 shows variation of daily averages of albedo, glacier surface temperature and wind speed during the study period. As the daily averaged glacier surface temperature increased towards 0°C (during some hours of the day the surface temperature reached 0°C, although the daily averaged surface temperature was lower than 0°C), the albedo of the glacier surface decreased, specifically during the months of November, December and January. Thus the melting glacier surface was one of the main reasons for the lowering of albedo values during this part of the season. Water absorbs more radiation compared to ice and so the melting glacier surface absorbs more radiation. Since melting increases with time during the summer there is a feedback loop to a continuous decrease of albedo. The other possible explanation for the declining albedo may be partial subsurface melting caused by solar radiation absorbed beneath the surface which may occur more often than surface melting. If some of the subsurface water percolates out of the ice, it enlarges air voids which scatter more light. Since these effects have not been measured or modelled it would be difficult to estimate their magnitude. An abrupt drop in the albedo value around 29 January 2008 was recorded despite the decreasing temperature trend. It may be because of a dust event after a long windy period (Fig. 5). The other reason for the continuous decline of the albedo may be the location of

https://doi.org/10.1017/S0954102009001989 Published online by Cambridge University Press

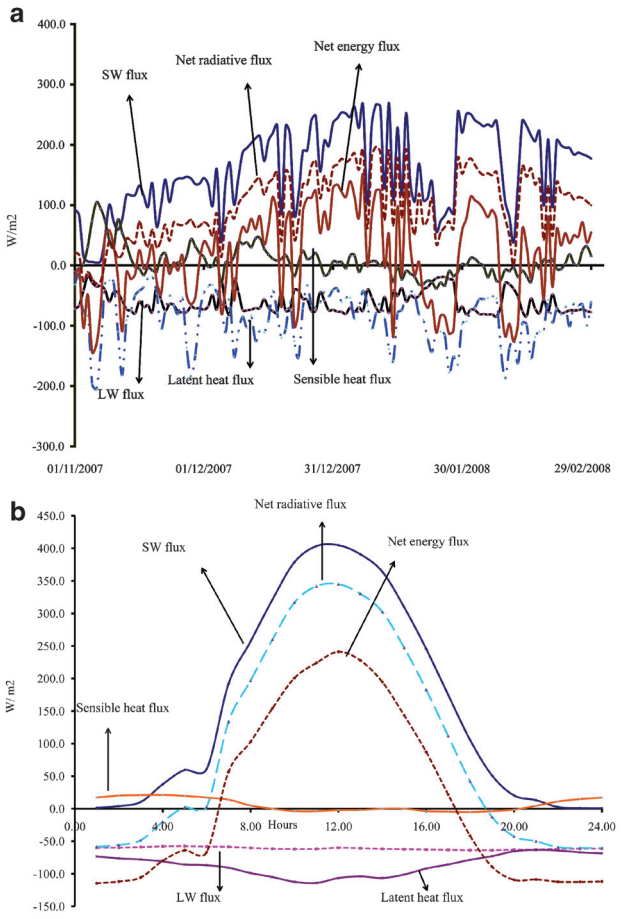

Fig. 6. a. Time series of daily averaged energy fluxes. **b.** Seasonal mean energy cycles.

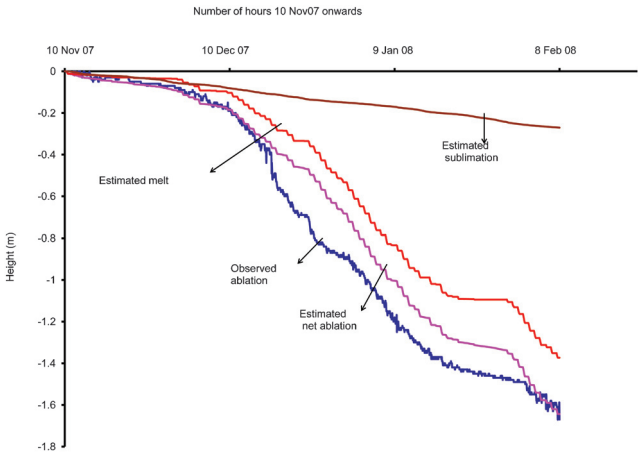

Fig. 7. Time series of observed and estimated ablation.

the AWS. The AWS was installed near an ice free area, so ice may be contaminated by wind-blown debris or some boulders or glacier debris may appear on the glacier surface after substantial melting of the ice in the later half of the summer season, causing more absorption of the radiation.

Time series of surface energy fluxes and ablation

Figure 6 shows a time series of daily averaged values of net shortwave flux, net longwave flux, sensible heat flux, latent heat flux and net energy balance at the glacier surface. Seasonal and monthly mean values of these fluxes are given in Table II. Net shortwave flux was the main source of the energy for the glacier with the seasonal mean value of 159 W m^{-2}. Large temporal variation was observed in the daily averaged net shortwave flux and varied from 6 W m^{-2} to 270 W m^{-2} (Fig. 6). Monthly mean of the net shortwave flux varied from 93 W m^{-2} for November to 187 W m^{-2} for February. The mean of the net shortwave flux was higher for the late summer months due to low albedo. The hourly net longwave flux varied from -16 W m^{-2} to -98 W m^{-2} and the daily average varied from -17 W m^{-2} to -85 W m^{-2} (Fig. 6) with the seasonal mean of -61 W m^{-2}. It shows the glacier surface is continuously losing energy in the form of longwave radiation. Hourly low values of the net longwave radiation were observed for cloudy sky conditions as the net longwave flux was strongly affected by the presence of cloud cover. Clouds re-emit the higher wavelengths of longwave radiation to the glacier surface compared to a clear sky and hence increase the significant magnitude of down-welling longwave radiation. Monthly mean net longwave flux varied from -54 W m^{-2} (January) to -68.6 W m^{-2} (February). A higher net longwave radiation loss by the glacier was observed for February despite it being the coldest month of the summer. The reason may be because it was the least cloudy month of the summer. Similarly, comparatively low longwave cooling was observed during January, as most of the days were cloudy. The net radiation or radiation balance is the sum of the net shortwave and the net longwave components. Net radiation flux was positive for most of the hours of the summer season with the seasonal mean value of 98 W m^{-2}, indicating a source of energy to the glacier surface.

Sensible heat flux arises as a result of temperature differences and wind over the glacier surface. The magnitude of the hourly estimated sensible heat flux varied from -86 W m^{-2} to 134 W m^{-2} and the daily averaged value from -38 W m^{-2} to 104 W m^{-2} (Fig. 7). Mean monthly values of the sensible heat flux varied from -9.2 W m^{-2} for January to 24 W m^{-2} for November, with little seasonal contribution to the net energy with an average value of 6.5 W m^{-2}. The sensible heat flux changes sign between different hours of the day is positive when the air temperature is higher compared to the glacier surface temperature and negative otherwise. The glacier surface temperature becomes higher than the air temperature after absorption of sufficient shortwave radiation around local solar noon (11h00 at the location) and the

https://doi.org/10.1017/S0954102009001989 Published online by Cambridge University Press

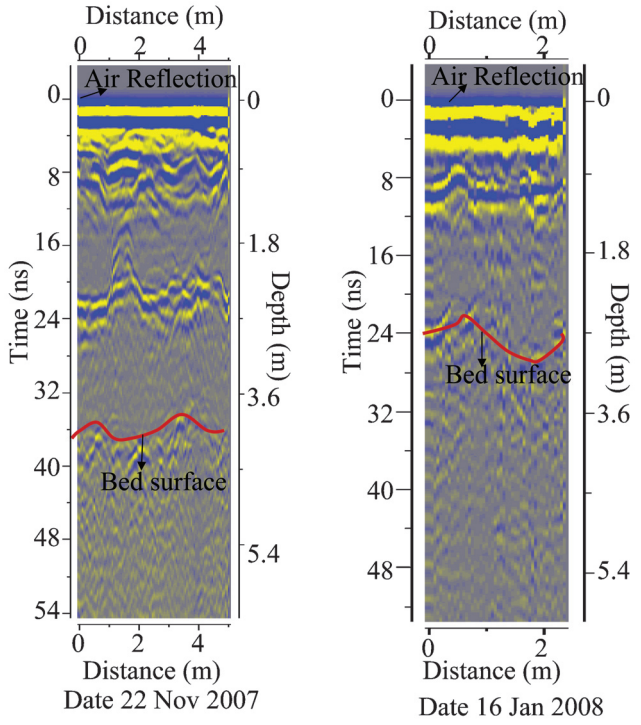

Fig. 8. Radargram of the GPR profiles.

gradient of sensible heat flux is then away from the glacier surface, resulting in loss of glacier energy.

Hourly magnitude of the latent heat flux varied from -300 W m^{-2} to 6 W m^{-2} and the daily averaged -24 W m^{-2} to -205 W m^{-2} with the seasonal mean of -86.7 W m^{-2}. Positive latent heat flux during some hours indicated deposition/condensation over the glacier surface. High values of latent heat flux were observed for all the summer months and the monthly mean varied from -79.7 W m^{-2} to -92.3 W m^{-2}. It indicates a high sublimation/evaporation rate from the glacier surface during the observation period. Hourly ice sublimation and ice melt was estimated and sublimation rate varied from zero to 0.00038 m w.eq. hr^{-1} (pure ice density of 917 kg.m^{-3} was used for the conversion) with the seasonal mean value of 0.00012 m w.eq. hr^{-1}, while estimated melt was up to 0.0064 m w.eq. hr^{-1}.

Daily estimated net energy flux showed large temporal variation and its magnitude varied from -140 W m^{-2} to 112 W m^{-2} with a seasonal average of 17.8 W m^{-2}. Monthly mean of net energy balance varied from -24.2 W m^{-2} for the month of November to 43.6 W m^{-2} for December. Except for November, the mean monthly value of net energy was positive. It indicates that sublimation is a dominant process in the net ablation of the glacier during November whereas it is melt for rest of the months. Figure 6 shows the average seasonal values of the various energy fluxes for 24 hours of the day. Net energy of the ice sheet is positive between 07h00–17h00 indicating melt as the dominant ablation process during these hours.

Figure 7 shows observed and estimated ablation of the glacier. Net estimated ablation has been derived from the sum of estimated sublimation and estimated melt for each hour (Fig. 7). Hourly glacier ablation values have been taken from ultrasonic sensor data. In the present paper ablation data from 10 November 2007–7 February 2008 has been used. In the radargram profiles of GPR (Fig. 8), an uneven bed surface of the glacier was identified and the net reduction in the glacier thickness between two GPR experiments conducted 15–20 days apart was calculated by averaging the depth of uneven bed surface. Radargram profiles of GPR on 22 November 2007 and 16 January 2008 (Fig. 8) show a reduction of 1.2 m in glacier thickness, which was comparable to the reduction of 1.3 m observed by the ultrasonic sensor during this period, recognizing the

Table III. Comparison of meteorological parameters and energy fluxes of various ice locations of Antarctica.

Ice location type:	Blue ice, Queen Maud Land	Dry Valley glacier, Taylor Valley	Glaciers of Antarctic Peninsula	Edge of the Antarctic ice sheet (present study site)
Elevation:	1170 m a.s.l	100–350 m a.s.l	150 m a.s.l	142 m a.s.l
Time period:	40 day average, summer period	average 22 Nov 1995–10 Jan 1996	mean 20 Dec 1994–21 Feb 1995	average 1 Nov 2007–29 Feb 2008
Parameters				
Air temperature (2 m) °C	-8.3	-	0.8	-2.2
Surface temperature °C	-7.0	-	-	-2.5
Wind speed (6 m) ms^{-1}	4.9 ± 3.7	-	-	-
Wind speed (2 m) ms^{-1}	-	-	4.6	6.2
Relative humidity (%)	-	-	70.1	53.3
Albedo	0.56	-	-	0.44
Net shortwave flux Wm^{-2}	127.9	115	-	159
Net longwave flux Wm^{-2}	-85.5	-66.5	-	-61
Net radiative flux Wm^{-2}	42.4	48.5	8.6	98
Sensible heat flux Wm^{-2}	-7.2	3.01	35.5	6.5
Latent heat flux Wm^{-2}	-28.7	-19.81	-25.5	-86.7
Subsurface heat flux Wm^{-2}	-6.5	1.49	-	-
Net energy flux Wm^{-2}	0	33.19	18.6	17.8

https://doi.org/10.1017/S0954102009001989 Published online by Cambridge University Press

uneven bed as a source of potential error. Ablation data for different months are given in Table II. Net 167 cm of glacier ice ablated from 10 November 2007–7 February 2008. Energy balance model estimates a net ablation of 164 cm during this period. There was a large variation between monthly observed and estimated net ablation. For December the model under-estimates the net ablation whilst for January it over-estimates. A good correlation coefficient ($r^2 = 0.97$) has been observed between hourly estimated ablation and observed ablation. In net estimated ablation, sublimation contributes 16.5% mass loss whilst the major contribution of 83.5% mass loss was from melt processes. Accumulation of new snow was nil. This study observed very high ablation (sublimation as well as melt) of the ice sheet in proximity to non-glaciated area of Schirmacher Oasis.

The Geological Survey of India (GSI) has been continuously monitoring the changes in the Dakshin Gangotri glacier snout (70°45'S, 11°34'E), near the present study area since 1983. The glacier tongue has shown continuous recession. The area vacated by the receding tongue from 1986–92 has been calculated as 5120 m^2 and an overall recession of 7 m has been observed during the decade 1983–93 (Asthana *et al*. 2002). The continuous recession of the glacier snout near Schirmacher Oasis also support the observations of the present study.

Comparison with other ice locations in Antarctica:

A comparison of the meteorological parameters and energy fluxes of the present study with other previous summer studies at various Antarctic locations (Lewis *et al*. 1998, Bintanja 1999, Schneider 1999) is shown in Table III. Net radiative flux and latent heat flux at the present location was higher compared with other locations. High net shortwave flux and low net longwave flux at the present location contribute to higher values of net radiative flux. The study location was windiest compared with previous study locations and that may be the reason for the observed high latent heat flux values. Sensible heat flux for a blue ice area (Bintanja 1999) was negative, while it was positive for other study sites. A higher value of sensible heat flux was observed for the glaciers of the Antarctic Peninsula. Net energy balance or energy available for melt was higher at the present location compared to blue ice area of Scharffenbergbotnen, Queen Maud Land, lower compared to a dry valley glacier, Taylor Valley, and comparable with glaciers of Antarctic Peninsula.

Conclusions

Net radiative flux was the main source of energy for the glacier while latent heat flux was the main heat sink. Net glacier energy balance was positive for the summer season of 2007–08 with a seasonal mean value of 17.8 W m^{-2}. The results show considerable ablation of the glacier near Schirmacher Oasis during this particular summer at a rate of 0.0172 m w.eq. day^{-1}. Mass balance of the ice sheet was -1.53 m w.eq. from 10 November 2007–7 February 2008. Zero accumulation was observed during this period. It was estimated that sublimation and melt processes contributes 16.5% and 83.5% to the net seasonal ablation respectively. There was a high correlation between estimated and observed glacier ablation, though the model under-estimates net ablation for December and over-estimates it for January. If a similar trend of ablation persists for a longer period the ice free area of the oasis will grow. Study of interannual climate variation over a longer period is needed to determine this. Energy balance study of the non-glaciated areas close to the ice sheet may also help in understanding the effect of warming of such areas on the ice sheet. Present study has highlighted the usefulness of GPR in the mass balance study of the glacier.

Acknowledgements

Authors are grateful to Dr R.N. Sarwade, Director Snow and Avalanche Study Establishment for permission to publish this paper. We are also thank the Defence Research and Development Organisation (DRDO) for funding the project. We express our sincere gratitude to NCAOR (National Centre for Antarctic and Ocean Research) and all the members of 26th Indian Scientific Expedition to Antarctica (especially H.S. Negi, SASE, S. Sownbowne, IITM and K. Jeeva, IIG) for extensive support during study. We would also like to thank Dr Timo Vihma, senior scientist of the Finnish Meteorological Institute, Finland for his valuable suggestions during the study. Comments by reviewers and the editorial team helped us immensely in improving the manuscript.

References

Ambach, W. & Kirchlechner, P. 1986. Nomographs for the determination of meltwater from ice and snow surfaces by sensible and latent heat. *Wetter Leben*, **38**, 181–189.

Asthana, R., Gaur, M.P. & Dharwadkar, A. 2002. Glaciological studies during the expedition. *Scientific Report of the Eighteenth Indian Expedition to Antarctica, Technical Publication*, No 16, 95–109.

Bintanja, R. 1995. The local surface energy balance of the Ecology Glacier, King George Island, Antarctica: measurements and modelling. *Antarctic Science*, **7**, 315–325.

Bintanja, R. 1999. On the glaciological, meteorological, and climatological significance of Antarctic blue ice areas. *Reviews of Geophysics*, **37**, 337–359.

Bintanja, R. & Reijmer, C.H. 2001. Meteorological conditions over Antarctic blue-ice areas and their influence on the local surface mass balance. *Journal of Glaciology*, **17**, 37–50.

Bintanja, R. & Van Den Broeke, M.R. 1994. Local climate, circulation and surface-energy balance of an Antarctic blue-ice area. *Annals of Glaciology*, **20**, 160–168.

Bintanja, R. & Van Den Broeke, M.R. 1995a. Momentum and scalar transfer coefficients over aerodynamically smooth Antarctic surfaces. *Boundary Layer Meteorology*, **74**, 89–111.

https://doi.org/10.1017/S0954102009001989 Published online by Cambridge University Press

BINTANJA, R. & VAN DEN BROEKE, M.R. 1995b. The surface energy balance of Antarctic snow and blue ice. *Journal of Applied Meteorology*, **34**, 902–926.

BRAUN, M. & SCHNEIDER, C. 2000. Characteristics of summer energy balance on the west coast of the Antarctic Peninsula. *Annals of Glaciology*, **31**, 179–183.

BROCK, B.W., WILLIS, I.C. & SHARP, M.J. 2006. Measurement and parameterization of aerodynamic roughness length variations at Haut Glacier d'Arolla, Switzerland. *Journal of Glaciology*, **52**, 281–297.

BROCK, B.W., WILLIS, I.C., SHARP, M.J. & ARNOLD, N.S. 2000. Modelling seasonal and spatial variations in the surface energy balance of Haut Glacier d'Arolla, Switzerland. *Annals of Glaciology*, **31**, 53–62.

CHOI, T., LEE, B.Y., KIM, S.-J., YOON, Y.J. & LEE, H.-C. 2008. Net radiation and turbulent energy exchange over a non-glaciated coastal area on King George Island during four summer seasons. *Antarctic Science*, **20**, 99–111.

FOUNTAIN, A.G., NYLEN, T.H., MACCLUNE, K.L. & DANA, G.L. 2006. Glacier mass balances (1993–2001), Taylor Valley, McMurdo Dry Valleys, Antarctica. *Journal of Glaciology*, **52**, 451–462.

GENTHON, C., LARDEUX, P. & KRINNER, G. 2007. The surface accumulation and ablation of a coastal blue-ice area near Cap Prudhomme, Terre Adelie, Antarctica. *Journal of Glaciology*, **53**, 635–645.

GREUELL, W. & KONZELMANN, T. 1994. Numerical modelling of the energy balance and the englacial temperature of the Greenland ice sheet: calculation for the ETH-camp location (West Greenland, 1155 m a.s.l). *Global and Planetary Change*, **9**, 91–114.

GUSAIN, H.S., NEGI, H.S. & KUMAR, M. 2008. *Temporal variability of the snow meteorological parameters over Antarctic continental ice sheet and estimation of surface energy budget, in Dronning Maud Land, East Antarctica*. Proceedings International workshop on snow, Glacier and Avalanches, IIT Mumbai. Delhi: Tata McGraw-Hill, 95–107.

HOFFMAN, M.J., FOUNTAIN, A.G. & LISTON, G.E. 2008. Surface energy balance and melt thresholds over 11 years at Taylor Glacier, Antarctica. *Journal of Geophysical Research*, **113**, 10.1029/2008JF001029.

KING, J.C. & TURNER, J. 1997. *Antarctic meteorology and climatology*. Cambridge: Cambridge University Press, 409 pp.

KING, J.C., ANDERSON, P.S. & MANN, G.W. 2001. The seasonal cycle of sublimation at Halley, Antarctica. *Journal of Glaciology*, **47**, 1–8.

LEWIS, K.J., FOUNTAIN, A.G. & DANA, G.L. 1998. Surface energy balance and meltwater production for a Dry Valley glacier, Taylor Valley, Antarctica. *Annals of Glaciology*, **27**, 603–609.

MISHRA, V.D. 1999. Albedo variations and surface energy balance in different snow-ice media in Antarctica. *Defence Science Journal*, **49**, 347–362.

PATERSON, W.S.B. 1994. *The physics of glaciers*, 3rd ed. Oxford: Elsevier, 480 pp.

PRATA, A.J. 1996. A new longwave formula for estimating downward clear-sky radiation at the surface. *Quarterly Journal of the Royal Meteorological Society*, **122**, 1127–1151.

PRICE, A.G. & DUNNE, T. 1976. Energy balance computation of snowmelt in a sub Arctic area. *Journal of Resource*, **12**, 686–694.

SCHNEIDER, C. 1999. Energy balance estimates during the summer season of glaciers of the Antarctic Peninsula. *Global and Planetary Change*, **22**, 117–130.

SRIVASTAVA, P.K. 2002. A comparative study of glacio-meteorological parameters, reflectance and surface energy exchange over different snow-ice media in Dronning Maud Land in East Antarctica. *Scientific Report of the Eighteenth Indian Expedition to Antarctica, Technical Publication*, No. 16, 153–190.

US ARMY CORPS OF ENGINEERS. 1956. *Summary report on the snow investigations - snow hydrology*. Portland, OR: North Pacific Division, Corps of Engineers, US Army, 434 pp.

UPADHYAY, D.S. 1999. *Cold climate hydrometeorology*. New Delhi: New AGE International, 218 pp.

VAN DEN BROEKE, M., REIJMER, C., VAN AS, D. & BOOT, W. 2006. Daily cycle of the surface energy balance in Antarctica and the influence of clouds. *International Journal of Climatology*, **26**, 1587–1605.

VAN DEN BROEKE, M.R., REIJMER, C.H., VAN DE WAL, R.S.W. & VAN AS, D. 2004. A study of the Anarctic surface energy and mass balance using automatic weather stations. *Journal of Geophysical Research*, **6**, 07593.

VAN DEN BROEKE, M., REIJMER, C., VAN AS, D., VAN DE WAL, R. & OERLEMANS, J. 2005. Seasonal cycles of Antarctic surface energy balance from automatic weather stations. *Annals of Glaciology*, **41**, 131–139.

VAUGHAN, D.G., BAMBER, J.L., GIOVINETTO, M., RUSSELL, J. & COOPER, A.P.R. 1999. Reassessment of net surface mass balance in Antarctica. *Journal of Climate*, **12**, 933–946.